50 Years Of Excellence

1972 - 2022

The International Maritime Transport and Logistics Conference

"MARLOG 12"

Sustainable & Innovative Technologies

Towards a Resilient Future

12 - 14 March, 2023 Alexandria - EGYPT

2023 12 Marlog

Presented by Dr Tahsin Tezdogan

Associate Professor in Maritime Engineering

University of Southampton

Hydrodynamic analysis of ship manoeuvrability at ports using CFD

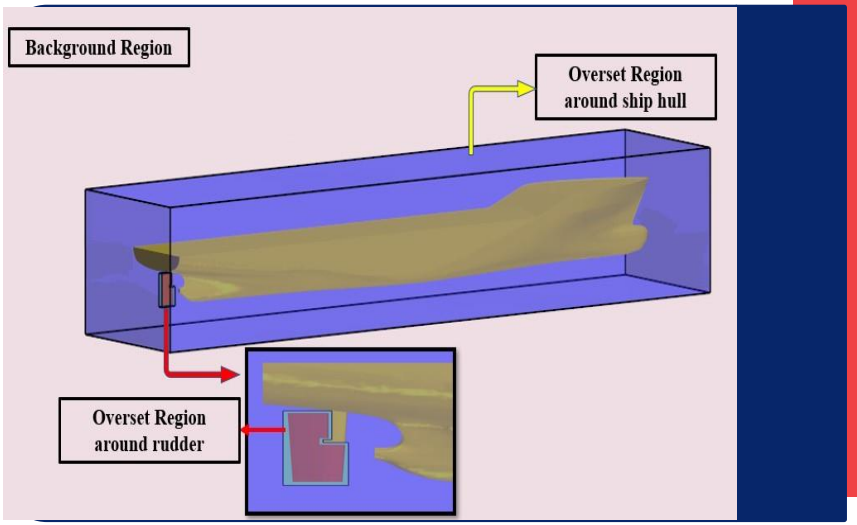

Introduction

The growing size of ships has highlighted the need to understand how they maneuver in shallow water. Navigation in shallow water is common for ships, especially when approaching harbors or ports.

Some coastal waters and open sea areas can also be considered shallow water regions with limited water depth. Proper decision-making about ship maneuvering actions requires a good understanding of a ship's maneuverability in shallow water by those in charge of navigation safety.

However, available information on ship maneuvering is usually limited to deep water, obtained through full-scale sea trials or model-scale experiments, in compliance with International Maritime Organization (IMO) standards.

Introduction

Although these provide information on a ship's maneuverability in deep unrestricted water, they do not offer practical insights into maneuvering in shallow water, which can differ significantly. This study aims to address this gap by investigating ship maneuvering performance in shallow water using an unsteady Reynolds-Averaged Navier Stokes (URANS) method.

In this study, the turning ability of the KCS model in shallow water ports is analyzed. The focus is on the maneuvering indices and hydrodynamic loads related to the turning movements. The study also evaluates the various hydrodynamic phenomena that occur during the maneuver to provide a better understanding of the turning behavior. As a result, this research could be beneficial in comprehending the complete maneuverability of a container ship model in various shallow water port environments.

Methodology

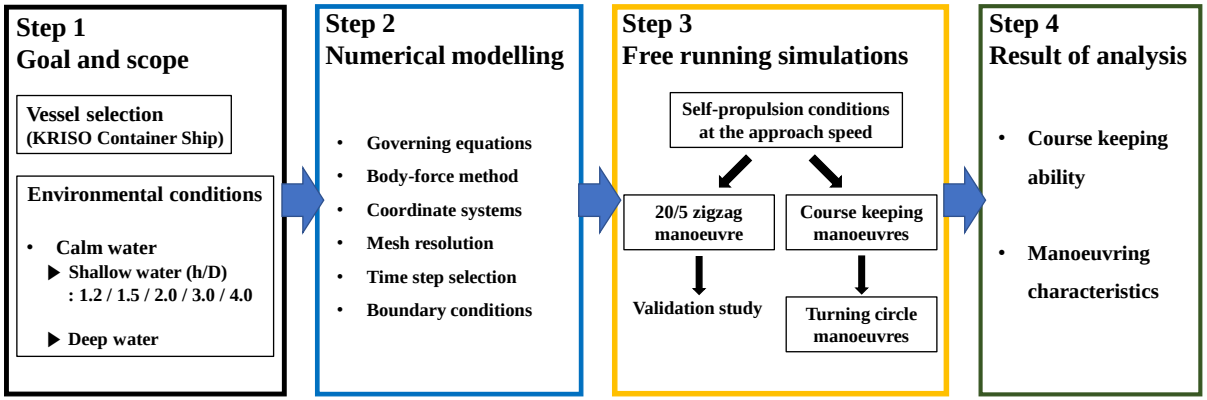

Proposed research methodology for the CFD free-running simulations

Step 1: Goal and scope

The objective of this study is to provide a comprehensive understanding of the impact of shallow water on ship maneuverability. The research will focus on:

Developing a CFD model for free-running maneuvers in a shallow water area such as ports,
Validating the CFD model using experimental data,
Analysing the effects of shallow water on ship maneuvrability (such as course keeping and turning capabilities).

Step 1: Goal and scope

The study conducted numerical simulations for the KCS model, which was developed by KRISO in Korea and had a scale factor of 75.24. The model was equipped with a semi-balanced rudder and an actuator disk.

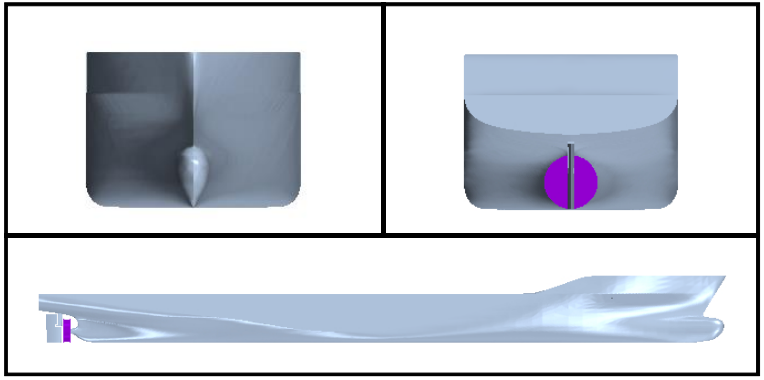

The KCS geometry with a semi balanced rudder and an actuator disk

The main dimensions of the KCS model

Main particulars	Symbols	Model scale (1:75.24)
Length between the perpendiculars	$L_{BP}(m)$	3.057
Length of waterline	$L_{WL}(m)$	3.0901
Beam at waterline	$B_{WL}(m)$	0.4280
Draft	$D(m)$	0.1435
Displacement	$\Delta(m^3)$	0.1222
Block coefficient	C_B	0.651
Ship wetted area with rudder	S (m^2)	1.6834
Longitudinal centre of buoyancy	$\%L_{BP}$, fwd+	-1.48
The metacentric height	GM(m)	0.008
Radius of gyration	K_{xx}/B	0.49
Radius of gyration	$K_{yy}/L_{BP}, K_{zz}/L_{BP}$	0.25
Propeller diameter	$D_P(m)$	0.105
Propeller rotation direction (view from stern)		Right hand side
Rudder turn rate	(deg./s)	20.1
Froude number	Fr	0.095
Reynolds number	Re	1.25×10^6

Step 1: Goal and scope

The study considered 7 different cases to be simulated in CFD, as shown below. The first case (Case 0) was a 20/5 modified zigzag maneuver in shallow water with a h/D ratio of 1.2, and the experimental results were used as a benchmark for validation.

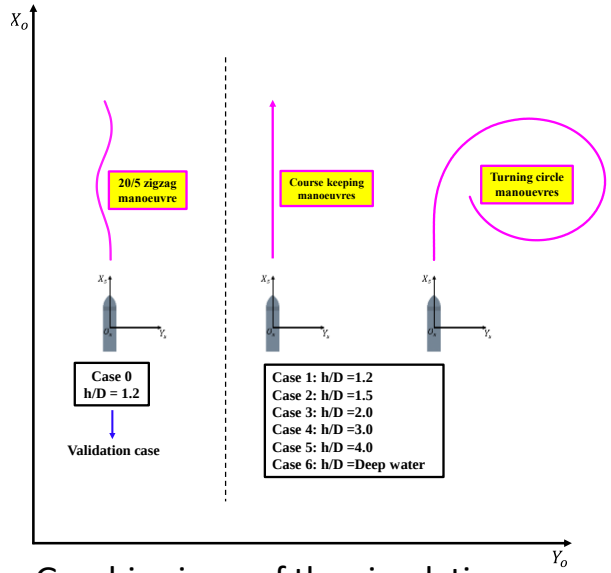

Graphic views of the simulation cases

The simulation cases

Case	Surge speed U_0 (m/s)	Propeller rev. (RPS)	Depth/draft h/D	Free running simulations
0	0.518	6.75	1.20	20/5 zigzag, starting to port (**Validation case**)
1	0.518	6.75	1.20	Course keeping, 35° starboard turn
2	0.518	6.56	1.50	Course keeping, 35° starboard turn
3	0.518	6.43	2.00	Course keeping, 35° starboard turn
4	0.518	6.28	3.00	Course keeping, 35° starboard turn
5	0.518	6.24	4.00	Course keeping, 35° starboard turn
6	0.518	6.07	Deep water	Course keeping, 35° starboard turn

Step 2: Numerical modelling

The study employed the commercial CFD package STAR-CCM+, version 15.04, for numerical simulations.

The ship propeller was modeled using a finite-thickness actuator disk based on the body force method, incorporating both axial and tangential forces in the flow field within the disk to mimic propeller behavior.

The computational domain was discretized using the Cartesian cut-cell method with the KCS model in STAR-CCM+. Six different grid generations were applied in the free-running simulations.

Step 2: Numerical modelling

The total mesh numbers for the free-running simulations

Case no.	Total cell number
0 (h/D=1.2)	8,854,466
1 (h/D=1.2)	8,854,466
2 (h/D=1.5)	8,968,119
3 (h/D=2.0)	9,580,662
4 (h/D=3.0)	9,950,540
5 (h/D=4.0)	10,287,254
6 (Deep water)	8,184,125

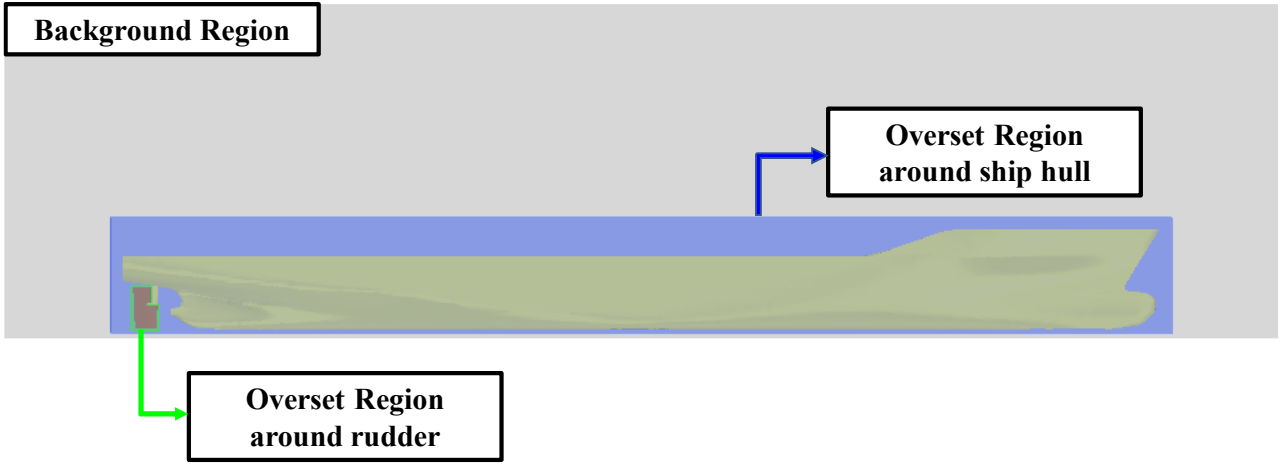

The illustration of the computational domain for the free-running CFD model

Step 2: Numerical modelling

In this study, all free-running CFD simulations satisfied the Courant-Friedrichs-Lewy (CFL) condition by maintaining a CFL number less than 1 for numerical stability. The ITTC (2014) recommends using $\Delta t \leq 0.01L/U$ for the time step (Δt) selection, with L and U being the ship length and speed, respectively. However, a more reliable level of accuracy for complex phenomena was achieved in this work by using a time step of **$\Delta t = 0.005s$**, which is ten times smaller than the recommended value.

Step 2: Numerical modelling

The shallow water simulations (Case 0-5) used velocity inlet boundary conditions at the upstream, side, and top boundaries to avoid velocity gradients, and a pressure outlet at the downstream boundary.

The bottom boundary was set as a stationary no-slip wall to represent the sea floor. Moving bodies (hull and rudder) had no-slip wall conditions.

To prevent wave reflection, wave damping with a length of 1.0 LBP was applied at the vertical boundaries. For deep-water simulation (Case 6), the only difference was the bottom boundary was set as a velocity inlet to represent deep water.

Step 3: Free running simulations

The 20/5 zigzag maneuver, the course keeping control, and the turning circle maneuver were performed for the KCS in this study. The control function for the modified 20/5 zigzag maneuver is as follows:

$$\delta(t) = \begin{cases} \min(kt, 20), \text{1st Rudder Execution} \ \ (t_1 \le t \le t_2) \\ \max(20 - k(t - t_2), -20), \text{2nd Rudder Execution} \ (t_2 \le t \le t_3) \\ \min(-20 + k(t - t_3), 20), \text{3rd Rudder Execution} \ (t_3 \le t \le t_4) \end{cases}$$

in which *t* is the time elapsed after the start of each rudder execution, δ(t) is the rudder angle, *k* is the maximum rudder rate (k = 20.1º/s). The ship was traveling straight at full speed when the rudder was first moved 20º to the port (1st rudder execution). This caused the ship to turn towards the port. When the ship had veered 5º off course, the rudder was moved 20º to the starboard (2nd rudder execution). This made the ship turn towards the starboard, slowing down its port ward turning until it reversed direction. Finally, when the ship reached 5º towards the starboard, the rudder was moved back to the port (3rd rudder execution).

Step 3: Free running simulations

A control module was designed to assess the ship's course-keeping ability:

$$\delta(t) = K_p e(t) + K_i \int_0^t e(t)dt + K_d \frac{de(t)}{dt}$$

$$e(t) = \psi(t) - \psi_c$$

where ψ(t) is the instantaneous yaw angle at a given time, Ψ_c is the target yaw angle which was defined at 0° to keep the ship in course. K_p, K_i, and K_d denote the proportional, integral, and derivative control gains, respectively. In this CFD set-up, the control gains were calculated by the trial-and-error method (K_p=5, K_i=0.05 and K_d=3). It is worth mentioning that the turning circle maneuver uses maximum rudder deflection (35°) to the starboard at maximum rudder rate and keeps the saturation rudder angle constant till the maneuver ends.

Results

Course keeping control

Ships at sea usually follow a navigation route of straight-line courses except for evasive maneuvers or planned course changes. This highlights the importance of evaluating a ship's ability to maintain a straight course, making it crucial to assess course-keeping behavior under various sea conditions for safe navigation.

Course keeping control

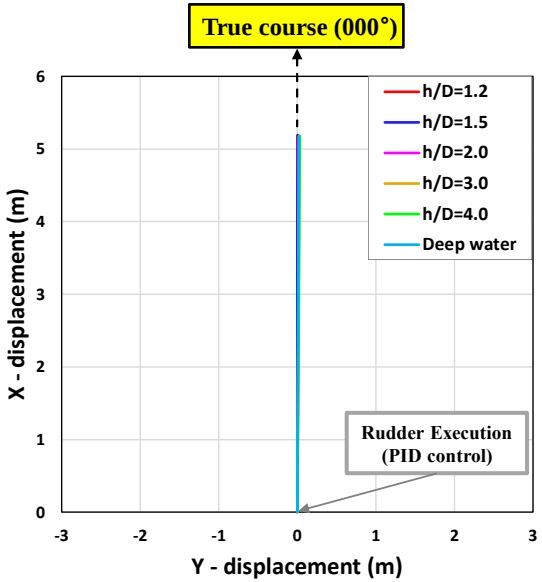

The mean values of the approach speed, ship resistance, vertical motions at the course keeping maneuver

Case no.	Approach speed U_0 (m/s)	Resistance F_x (N)	Heave (m)	Pitch (degrees)
1 ($h/D = 1.2$)	0.518	1.913	0.0033	0.165
2 ($h/D = 1.5$)	0.518	1.669	0.0024	0.166
3 ($h/D = 2.0$)	0.518	1.474	0.0017	0.169
4 ($h/D = 3.0$)	0.518	1.367	0.0011	0.172
5 ($h/D = 4.0$)	0.518	1.323	0.0008	0.172
6 (Deep water)	0.518	1.204	0.0004	0.171

The comparison of the trajectories practiced by the ship at the course keeping manoeuvre

Turning circle maneuver

The standard turning circle maneuver involves the ship sailing forward under self-propulsion, then the rudder being deflected to a hard-over angle of 35° to the starboard side, at a maximum rate of 20.1°/s. This causes the ship to turn in the starboard direction. The simulations end when the ship's heading angle reaches 360°, as per the procedure outlined by IMO (2002). The simulation time varies based on the ship's yaw velocity during the maneuver. The ship's turning behavior is assessed using standard parameters such as advance, transfer, tactical diameter, and time to 90°/180° heading changes.

Turning circle maneuver

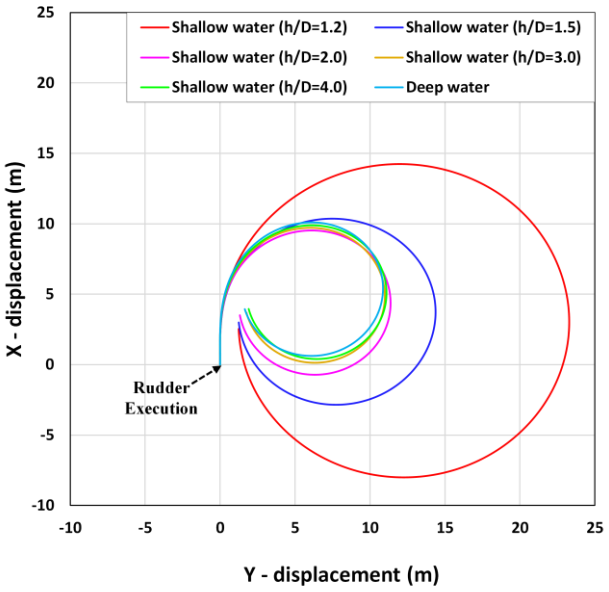

The predicted turning trajectories for all cases

CFD results for the turning parameters

Parameters (CFD results)	Case 1 (h/D=1.2)	Case 2 (h/D=1.5)	Case 3 (h/D=2.0)	Case 4 (h/D=3.0)	Case 5 (h/D=4.0)	Case 6 (Deep)
Advance (m)	14.23 **$(4.66L_{BP})$**	10.33 **$(3.38L_{BP})$**	9.45 **$(3.09L_{BP})$**	9.57 **$(3.13L_{BP})$**	9.73 **$(3.18L_{BP})$**	9.89 **$(3.24L_{BP})$**
Transfer (m)	11.56 **$(3.78L_{BP})$**	6.82 **$(2.23L_{BP})$**	5.16 **$(1.69L_{BP})$**	4.80 **$(1.57L_{BP})$**	4.80 **$(1.57L_{BP})$**	4.65 **$(1.52L_{BP})$**
Time for yaw 90 degrees (s)	47.24	32.51	27.97	27.64	27.92	28.04
Tactical diameter (m)	23.28 **$(7.62L_{BP})$**	14.34 **$(4.69L_{BP})$**	11.29 **$(3.69L_{BP})$**	10.85 **$(3.55L_{BP})$**	10.94 **$(3.58L_{BP})$**	10.67 **$(3.49L_{BP})$**
Time for yaw 180 degrees (s)	93.88	64.51	55.38	54.49	54.78	55.21

Turning circle maneuver

According to Yeo et al. (2016):

Turning maneuvers resulted in a slower change in the ship's heading angle in shallower water depths.

The ship performing turning maneuvers experienced increasing hydrodynamic forces as the ratio of water depth to draft decreased exponentially.

Smaller h/D ratios were found to result in increased turning parameters such as ship advance, transfer, and tactical diameter.

Conclusions

Key findings:

The maneuvering vessel at ports (i.e., in restricted waters) exhibited reasonably well “course-keeping control”, as shown by its real sailing courses being steady with the real course. This indicates that the restricted depths have little impact on “course keeping” when there are **no** outside disturbances such as waves.

The study emphasized the impact of restricted depth on the ship's turning behavior by comparing the so-called critical turning factors and hydrodynamic properties with h/D ratios. Decreasing h/D led to increased ship advance, transfer, and tactical diameter.

Thank You